Pergamon

Geochimica et Cosmochimica Acta, Vol. 66, No. 5, pp. 783–795, 2002

0016-7037/02 $22.00 + .00

PII S0016-7037(00)00821-3

Sorption of chromate ions diffusing through barite-hydrogel composites: Implications for the fate and transport of chromium in the environment

MANUEL PRIETO,* ÁNGELES FERNÁNDEZ-GONZÁLEZ, and RUT MARTÍN-DÍAZ
Departamento de Geología, Universidad de Oviedo, 33005 Oviedo, Spain

(*Received January* 16, 2001; *accepted in revised form August* 16, 2001)

Abstract—The interaction of Cr(VI) with barite is studied by quantifying the effect of this mineral on the net flux of chromate ions diffusing through an artificial porous medium consisting of barite grains embedded in a matrix of silica hydrogel. The gel suppresses convection and advection, only allowing diffusion of the aqueous ions, which eventually can be sorbed on the surface of the embedded grains. We find that long-term Cr(VI) uptake by barite occurs by epitaxial overgrowth of a $Ba(CrO_4,SO_4)$ solid solution with the barite structure. In these particular experiments, the epitaxial crystallites have compositions around $BaCr_{0.89}S_{0.11}O_4$. Sorption on barite reduces the net flux of chromate ions in relation to the flow through an equivalent (with the same porosity and tortuosity) but unreactive quartz-gel composite. A linear sorption model with a factor K_d = 0.291 was used to account for the experimental results. This factor is a complex measure that depends on the bulk medium characteristics and on the tendency of CrO_4^{2-} to partition into barite under the precipitation conditions. Here, we assess the operating precipitation conditions in terms of possible limiting scenarios of supersaturation and discuss their influence on the partitioning of CrO_4^{2-} ions into barite. The results demonstrate that precipitation of $Ba(SO_4,CrO_4)$ solid solutions may be an option to control the concentration of Cr(VI) in natural waters. Neglecting to consider such solid solution formation will lead to overestimates of the availability and mobility of Cr(VI) in the environment. *Copyright © 2002 Elsevier Science Ltd*

1. INTRODUCTION

The interaction of dissolved toxic metals with mineral surfaces influences their transport behavior in soils and groundwater systems. In general, the net flux of metals is reduced by sorption on the surface of soil minerals or aquifer sands (Davis et al., 1987; Fuller and Davis, 1987; Dudley et al., 1988; Reeder, 1996). Sorption is, in abstract terms, the change in concentration of a chemical in the solid matter as a result of mass-transfer among solution and solid. Metals can be sorbed by true adsorption, by absorption or diffusion into the solid, or by surface precipitation to form a metal-bearing adherent phase that may consist of chemical species derived from both the aqueous solution and dissolution of the solid (Sposito, 1986). Macroscopic studies of uptake of metals by minerals are mainly focused to determine sorption isotherms (Zachara et al., 1991; Brown et al., 1995). Measurements of sorption kinetics are usually carried out in agitated reactors, where an aqueous solution containing the pollutant is placed in contact with single-phase mineral solids. The influence of the sorption processes on the immobilization of toxic metals is always in the background of these experiments, but direct experimental studies about the reactive-transport of metals through interacting porous media are rare. Moreover, because the amount of material sorbed is small relative to the amount of sorbing solids, unambiguous characterization of the identity and stoichiometry of the sorbed entities, their growth mechanisms and their crystallographic relations to the substrate may be extremely tedious, if not impossible. These uncertainties are being reduced by the introduction of near-surface sensitive techniques (Stipp et al., 1992; Chiarello et al., 1997), but the fact that disparate models are argued to account for the same process indicate that there is a clear need for improved experimental methods.

The present work tries to overcome these difficulties by improving the size of the "sorbed individuals," which is possible when sorption occurs by surface precipitation of a metal-bearing solid. With this aim, we have studied the transport of dissolved metals through artificial porous media consisting of mineral grains embedded in a matrix of silica hydrogel. This gel matrix contains ~95 wt% water within interconnecting pores separated by a sheetlike structure. The gel suppresses convection and advection, only allowing diffusion of the aqueous ions, which eventually can be sorbed on the surface of the embedded minerals.

From experimental data, it is abundantly clear that gels reduce the nucleation probability (Henisch, 1988; Lefaucheux and Robert, 1994; Prieto et al., 1994), and in that sense, they offer certain research opportunities that crystallization from "free" aqueous solutions cannot provide. So in the context of purposeful crystal growth, the suppression of nucleation is the principal function of the gel because a lower nucleation density favors the development of larger crystals. Similarly, in the context of the present experiments, the gel yields a drastic decrease in the surface nucleation density and, consequently, a significant increase in the size of the precipitating individuals. This increase allows characterizing the sorbed phase and its crystallographic relation to the substrate. Moreover, the method allows determining the effectiveness of the sorption process from diffusivity measurements. Here, we illustrate this method for the diffusion of CrO_4^{2-} ions through barite-gel composites.

As a result of its widespread industrial use, chromium is present in many soils, sediments, and natural waters that have been subjected to pollution (Nriagu, 1988). In particular, hexavalent chromium Cr(VI) is a toxic soluble anion (CrO_4^{2-});

* Author to whom correspondence should be addressed (mprieto@asturias.geol.uniovi.es).

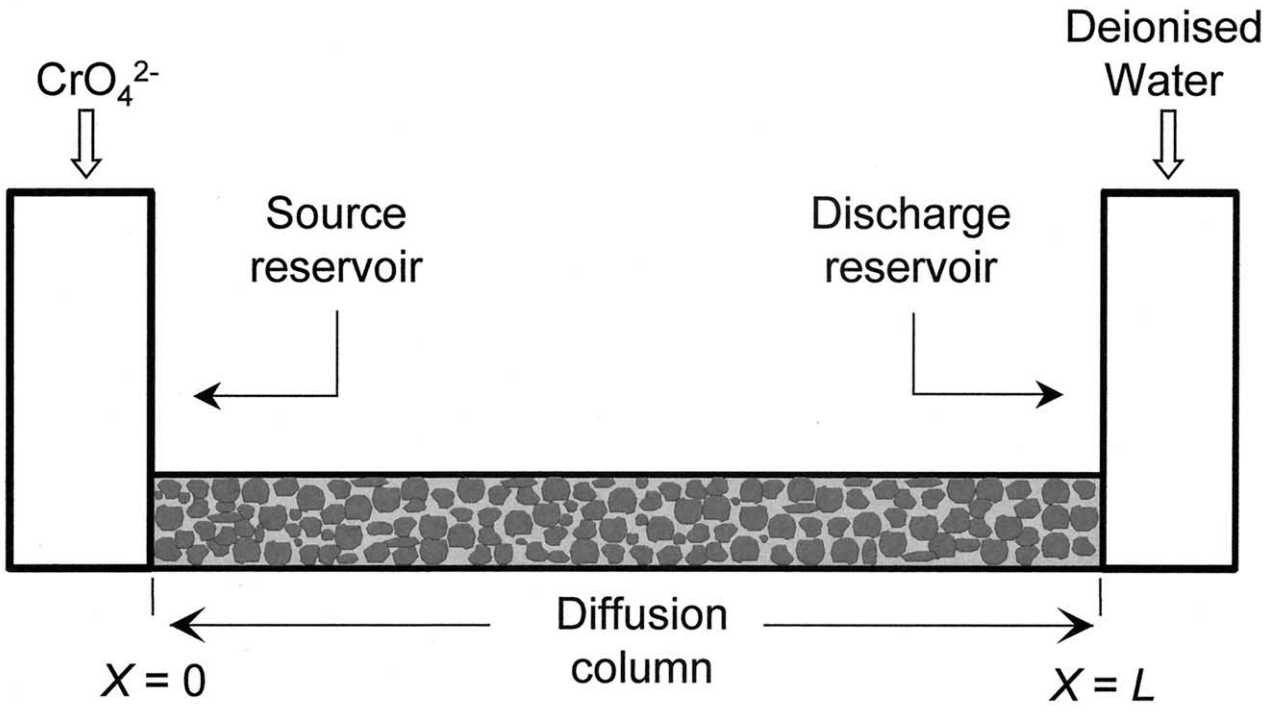

Fig. 1. Schematic representation of the experimental U-tube arrangement. Two solution reservoirs are separated by a diffusion column consisting of mineral grains embedded in a matrix of silica hydrogel. The source reservoir was filled with a parent solution of the toxic metal and the discharge reservoir with deionized water.

trivalent chromium Cr(III) is a much less toxic cation (Cr^{3+}) that has a strong affinity for particle surfaces (Peterson et al., 1997). Therefore, environmental remediation of sites contaminated by chromium usually involves reduction of Cr(VI) to the less mobile and toxic Cr(III) (Sedlak and Chan, 1997; Pettine et al., 1998). However, partial immobilization of aqueous Cr(VI) could be carried out directly, without reduction to Cr(III), by sorption of CrO_4^{2-} ions on the surface of barite crystals. In fact, barium chromate and barium sulfate form a complete solid solution series, where CrO_4^{2-} ions substitute for SO_4^{2-} in the barite structure (Fernández-González et al., 1999). Both end members are isomorphous and crystallize in the same space group Pnma (Miyake et al., 1978; Hauff et al., 1983). As a consequence, sorption of CrO_4^{2-} ions on barite crystals could occur by surface precipitation of $Ba(CrO_4,SO_4)$ solid solutions.

2. EXPERIMENTAL METHODS

2.1. Experimental Device

The experimental arrangement used in this work is simple and has been used with different modifications as a method of growing crystals in gels (Henisch, 1988; Prieto et al., 1990, 1994). Figure 1 shows a typical U-tube arrangement in which two reservoirs are separated by a diffusion column. For the experiments performed in this work, the diffusion column is a composite that consists of mineral grains embedded in a matrix of polymerized silica gel. To prepare the diffusion column, the horizontal branch of the U-tube was completely filled with mineral grains immersed in a sodium silicate (Na_2SiO_3) aqueous solution acidified with HCl 1 N. After some minutes, this solution polymerizes to form a gel that agglutinates the grains. The silica hydrogel is a porous medium with a sheetlike structure that forms interconnecting cells (Henisch, 1988). In the gel, the pore network is not uniform, although the overall porosity and the water content depend on the concentration of the sodium silicate solution used and on the initial pH. For the Na_2SiO_3 solution used here (Merck, density: 1.059 g cm^{-3}; pH 11.2) acidified with 1N HCl to a pH = 5.5, the "effective water" in the gel is ~95.6 wt% and the pores have diameters from less than 0.1 μm up to 0.5 μm. This structure allows the gel to be used as a transport medium where convection and advection are suppressed, only allowing the diffusion of the aqueous ions, which occasionally can be sorbed on the surface of the embedded mineral grains.

As shown in Table 1, two different kinds of mineral-gel composites were used. The first consists of barite grains with diameters ranging from 1 mm up to 1.5 mm, and the second was made of quartz grains with diameters in the same range. Quartz grains were anhedral frag-

Table 1. Characteristics of the barite-gel and quartz-gel diffusion columns. In both cases, the diffusion column was a cylinder of 9.048 cm^3.

Composite	Grain size (mm)	Volume of mineral in column (cm^3)	Volume of hydrogel in column (cm^3)	Volume of pore fluid in column (cm^3)	Porosity
Barite gel	$1 < Ø < 1.5$	4.37	4.68	4.54	0.494
Quartz gel	$1 < Ø < 1.5$	4.30	4.75	4.47	0.502

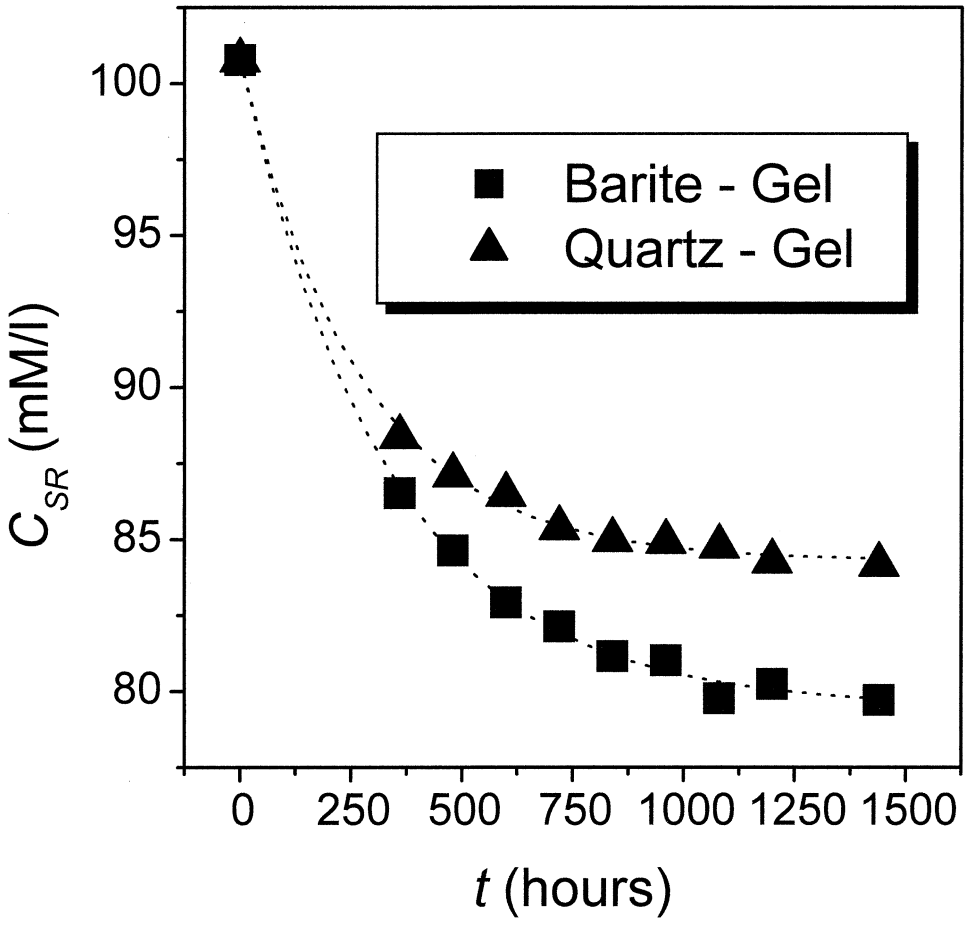

Fig. 2. Concentration evolution in the source reservoir for barite-gel (squares) and quartz-gel (triangles) diffusion columns. The experimental data points have been fitted to an exponential decay function (Eqn. 1).

ments prepared from high-grade quartz single crystals. Barite grains were subhedral fragments dominated by {001}, with {210} and {010} as minor cleavage surfaces. In both cases, the mineral grains were ultrasonically cleaned in deionized water. The diffusion column was a cylinder of 9.048 cm^3 with a length of 8 cm and a diameter of 1.2 cm. The amount of gel and mineral grains required to completely fill this cylinder is shown in Table 1. The porosity is slightly different for quartz-gel and barite-gel composites, but the effective tortuosity is assumed to be the same. This assumption is reasonable if one considers that aqueous diffusion only occurs through the interconnecting cells in the identical gel matrix, and that both composites have practically the same mineral/gel volume ratio and the same size distribution.

2.2. Diffusion Experiments

Diffusion experiments were carried out by filling the "source reservoir" (see Fig. 1) with 12 cm^3 of a 0.1 M Na_2CrO_4 aqueous solution and the "discharge reservoir" with 12 cm^3 of deionized water. When the experiment starts, the diffusion column is free of pollutant, but gradients in Cr concentration develop as diffusion time passes by. As a consequence, the pollutant concentration decreases in the source reservoir and increases in the discharge reservoir with diffusion time. This evolution was quantified by terminating diffusion experiments at fixed time intervals, removing the whole solutions from the reservoirs, and analyzing them for chromium. Obviously, this method involves carrying out a set of identical experiments (with different duration) for each kind of mineral-gel composite. For each diffusion time, the experiment was repeated 5 times. So the values represented in Figures 2 and 3 are average values corresponding to five analogous experimental runs. In sum, a total of 90 experiments (nine diffusion times $\times$ five runs $\times$ two composites) and 180 analyses (one for each reservoir) were carried out. Moreover, two single diffusion experiments were carried out starting from 0.15 and 0.2 mol/L parent solutions. Both experiments were stopped after 960-h diffusion time.

Analyses of chromium were carried out by inductively coupled plasma mass spectrometry (HP-4500) with ^{59}Co as internal standard, with a detection limit of 0.02 ng ml^{-1}. Additionally, some analyses were carried out to estimate the discharge of barium (resulting from the dissolution of the barite grains) to the reservoirs. Reagent grade chemicals (Merck) and deionized water (MilliQ) were used in all cases. During the experiments the temperature was maintained to 25 $\pm$ 0.1°C. After the diffusion experiments, some grains were extracted from the column to verify the incorporation of chromium on their surface. With this aim, X-ray dispersive-energy microanalyses of the grain surfaces were carried out in a scanning electron microscope (JEOL, JSM-LINK-6100).

3. RESULTS

3.1. Concentration Evolution in the Solution Reservoirs

Figures 2 and 3 show the concentration evolution in the reservoirs for the two kinds of diffusion columns (composites) used in this work. As expected, the concentration in the source reservoir decreases with diffusion time t, whereas it increases in the discharge reservoir. As can be observed in Figure 2, the

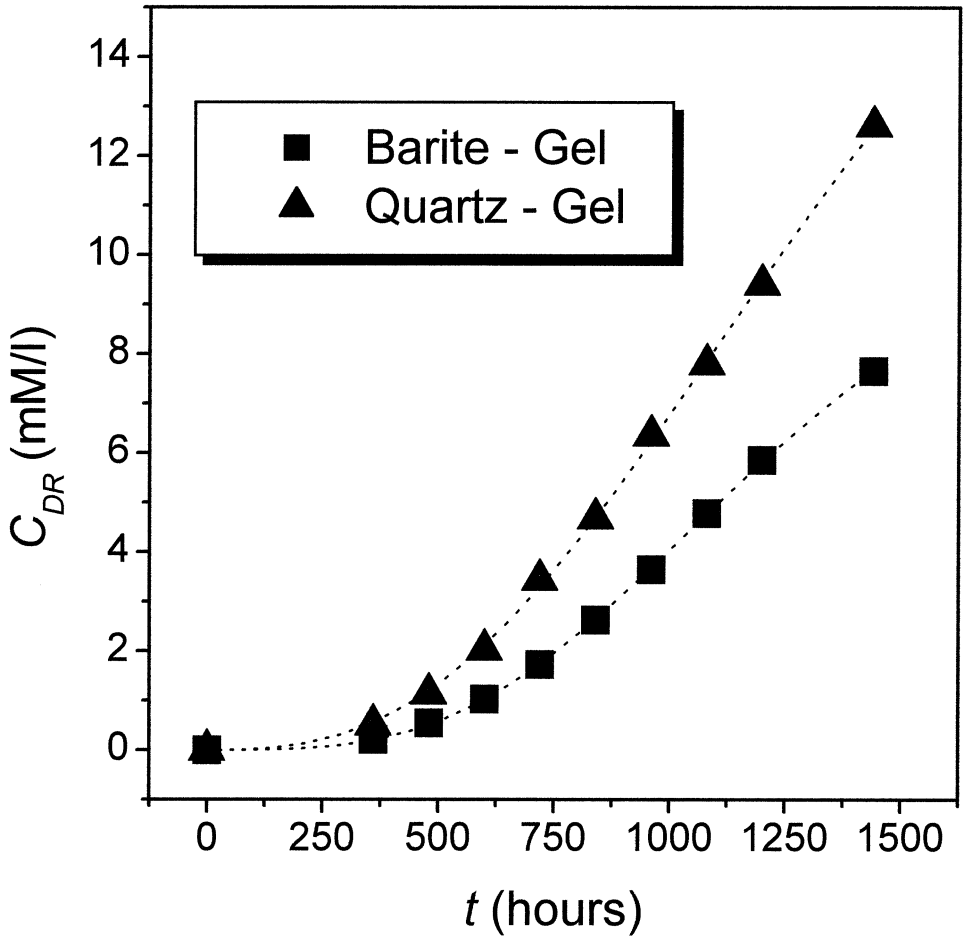

Fig. 3. Concentration evolution in the discharge reservoir for barite-gel (squares) and quartz-gel (triangles) diffusion columns. The experimental data points have been fitted to a sigmoidal function (Eqn. 2).

concentration C_{SR} in the source reservoir (x = 0) decays with t in an exponential way. In both cases, the data points have been fitted to an empirical function

$$C_{SR}(t) = C(0, t) = C_0 - A_1 + A_1 \times \exp\left(\frac{-t}{A_2}\right), \quad (1)$$

where A_1 and A_2 are fitting parameters and C_0 is the initial concentration of the source reservoir; that is, $C_0 = C_{SR}(0) = C(0,0)$. The fitting parameters corresponding to the data points in Figure 2 are shown in Table 2. The concentration decay in the source reservoir is more rapid for the composite made of barite.

Figure 3 shows the evolution of concentration C_{DR} in the discharge reservoir (x = L). In this case, the data series can be fitted to a sigmoidal empirical function, namely

$$C_{DR}(t) = C(L, t) = \frac{-B_1}{1 + \left(\frac{t}{B_2}\right)^{B_3}} + B_1, \quad (2)$$

where B_1, B_2, and B_3 are fitting parameters. Table 3 displays these parameters for the data series obtained in this work. Obviously, Eqn. 2 satisfies the condition $C_{DR}(0) = 0$.

As can be observed, the increase of concentration in the discharge reservoir is significantly more rapid for quartz-gel composites. Although the concentration-time data series are not strictly comparable because both kinds of composite have slightly different porosities, this faster increase for quartz-gel composites roughly indicates an important removal of this pollutant from the aqueous phase when diffuses through barite-gel composites. In fact, quartz grains seem to be quite unreactive for chromate ions, whereas significant sorption phenomena can be observed on the surface of barite crystals.

In the case of barite-gel composites, the discharge of barium and sulfate resulting from dissolution of barite towards the reservoirs seems to be fairly insignificant. The concentration of

Table 2. Source reservoir: fitting of time-concentration data to Eqn. 1.

Composite	A_1	Error	A_2	Error
Barite gel	21.291	0.182	332.890	10.762
Quartz gel	16.487	0.124	271.244	9.618

Table 3. Discharge reservoir: fitting of time-concentration data to Eqn. 2.

Composite	B_1	Error	B_2	Error	B_3	Error
Barite gel	12.514	0.279	1251.689	17.616	3.296	0.0478
Quartz gel	25.255	1.819	1445.301	72.082	2.721	0.0884

barium in the discharge reservoir was always less than 0.02 ppm. This means that in the gel, barite dissolution is a slow process. Moreover, as discussed below, this discharge is inhibited by precipitation of $Ba(SO_4,CrO_4)$.

3.2. Sorption of CrO_4^{2-} on Barite: Nature and Configuration of the Sorbed Entities

Figure 4 shows, at three different scales, images of a typical (001) surface of a barite grain taken after diffusion of CrO_4^{2-} ions through a barite-gel composite. The surface evidences clear dissolution signs and is covered by innumerable small crystals, with a higher nucleation density at the more reactive cleavage macrosteps. These crystallites show the typical morphologies of chromium-rich $Ba(CrO_4,SO_4)$ crystals grown in gels (Fernández-González et al., 1999). In this particular case, dispersive-energy microanalyses yield compositions around $BaCr_{0.89}S_{0.11}O_4$. The nuclei compositions can vary depending on the location of the barite grain in the diffusion column, but always in a narrow range ($\pm$ 0.04) close to $X_{BaCrO_4} = 0.89$. It is also worth noting that experiments carried out starting form Na_2CrO_4 parent solutions with different initial concentrations (0.15 and 0.2 mol/L) lead exactly to the same results—that is, no significant variation has been observed in the composition of the precipitates.

Nucleation occurs in a nonrandom orientation with a strict parallelism between crystallographic directions of substrate and overgrowing crystals, as shown in Figure 5. This is to be expected if one considers that barite and barium chromate form a nearly ideal solid solution series, where the lattice parameters depend in a linear way on the composition (Fernández-González et al., 1999): heterogeneous nucleation is favored by close lattice match, and close lattice match leads to oriented overgrowth or epitaxy. In this case, the lattice misfit $f_{[100]}$ along [100] is

$$f_{[100]} = (a_o - a_s)/a_s = 2.33\%, \tag{3}$$

where a_s = 8.881 Å and a_o = 9.088 Å are, respectively, the [100] lattice parameters for substrate ($BaSO_4$) and overgrowth ($BaCr_{0.89}S_{0.11}O_4$). The misfit along [010] is even lower ($f_{[010]}$ = 1.17%). Cleavage macrosteps are more active sites for nucleation because they enable more of the surface of the nucleus to be in contact with the substrate and hence lower its total surface energy. Moreover, the lattice misfit along [001] is fairly low ($f_{[001]}$ = 1.90%), and nucleation at the cleavage macrosteps can permit lattice match in all three dimensions.

In contrast to barite, the surface of the quartz grains remains perceptibly free of chromium after diffusion of CrO_4^{2-} ions through a quartz-gel composite. In practice, the presence of chromium on the quartz grains was not detected after numerous and careful X-ray microanalyses. So it seems that sorption of chromium on quartz is negligible compared with sorption on barite.

4. DISCUSSION

According to the previous observations, the epitaxial overgrowth of a barium sulfate-chromate solid solution seems to be the most effective mechanism of uptake of chromium by barite. In the present scenario, such a mechanism involves (1) the arrival of diffusing ions (CrO_4^{2-}) near the mineral surface, (2) the release of solute (Ba^{2+} and SO_4^{2-}) from the mineral surface to the pore fluid, and (3) the reaction between the released solute and the diffusing CrO_4^{2-} to form solid-solution nuclei. Thus, barite dissolution coexists with surface precipitation of $Ba(CrO_4,SO_4)$, resulting in a mechanism of sorption by coprecipitation.

When diffusion is accompanied by sorption, the usual equation for diffusion in one dimension has to be modified to allow for this, and becomes (Crank, 1975)

$$\frac{\partial C(x,\,t)}{\partial t} = \bar{D}\frac{\partial^2 C(x,\,t)}{\partial x^2} - \frac{\partial S(x,\,t)}{\partial t}, \tag{4}$$

where S(x,t) is the loss of pollutant concentration in the pore fluid and $\bar{D}$ is the "effective" diffusion coefficient of the pollutant in the composite. Solute diffusion in porous media is hindered by the tortuous nature of the pores and by the diminished cross-sectional area available for diffusion (Grathwohl, 1998). Therefore, $\bar{D}$ is related to the diffusion coefficient in a free solution through a formation factor, $\phi\tau_e^2$, which depends on both the porosity ϕ and the effective tortuosity τ_e of the porous medium. The effective tortuosity comprises all factors that alter diffusional transport in porous media including pore-throat constrictions, isolated pores, etc. (Oelkers, 1996). If one assume a linear relation ($S = K_d C$) between the concentration S of immobilized pollutant and the concentration C of pollutant free to diffuse—which is reasonable when sorption occurs via formation of an adherent layer of solid solution (Tesoriero and Pankow, 1996)—on substituting for S from Eqn. 4 we have

$$\frac{\partial C}{\partial t} = \frac{\bar{D}}{1 + K_d}\frac{\partial^2 C}{\partial x^2}, \tag{5}$$

which is seem to be the usual form of equation for diffusion governed by a transient "apparent" diffusion coefficient given by $D_a = \bar{D}/(1 + K_d)$—that is,

$$\frac{\partial C}{\partial t} = D_a\frac{\partial^2 C}{\partial x^2}. \tag{6}$$

Clearly, the effect of the sorption reaction is to reduce the net flux of pollutant. Hence, D_a may be interpreted as a "retarded" pore diffusion coefficient and $\Re = 1 + K_d$ may be termed "retardation factor." Obviously, sorption does not alter the

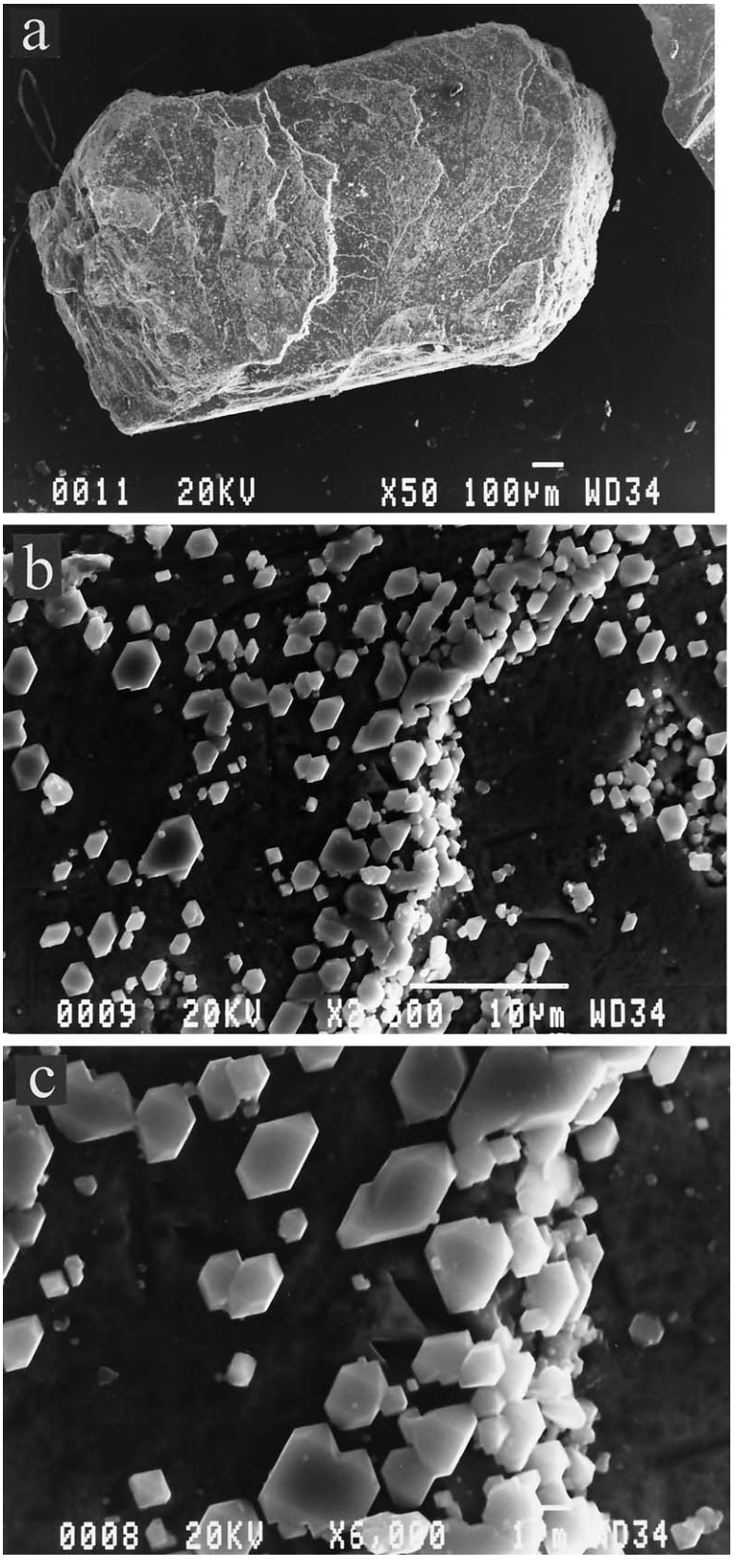

Fig. 4. (a) Scanning electron micrograph of a barite grain extracted from the gel after diffusion of CrO_4^{2-} ions. (b, c) Details of the (001) surface showing the oriented overgrowth of $Ba(CrO_4,SO_4)$ crystals. In (b), a cleavage macrostep (completely covered by aligned crystallites) goes from the upper to the lower central part of the figure. A detail of this macrostep can also be observed in (c) at a higher magnification.

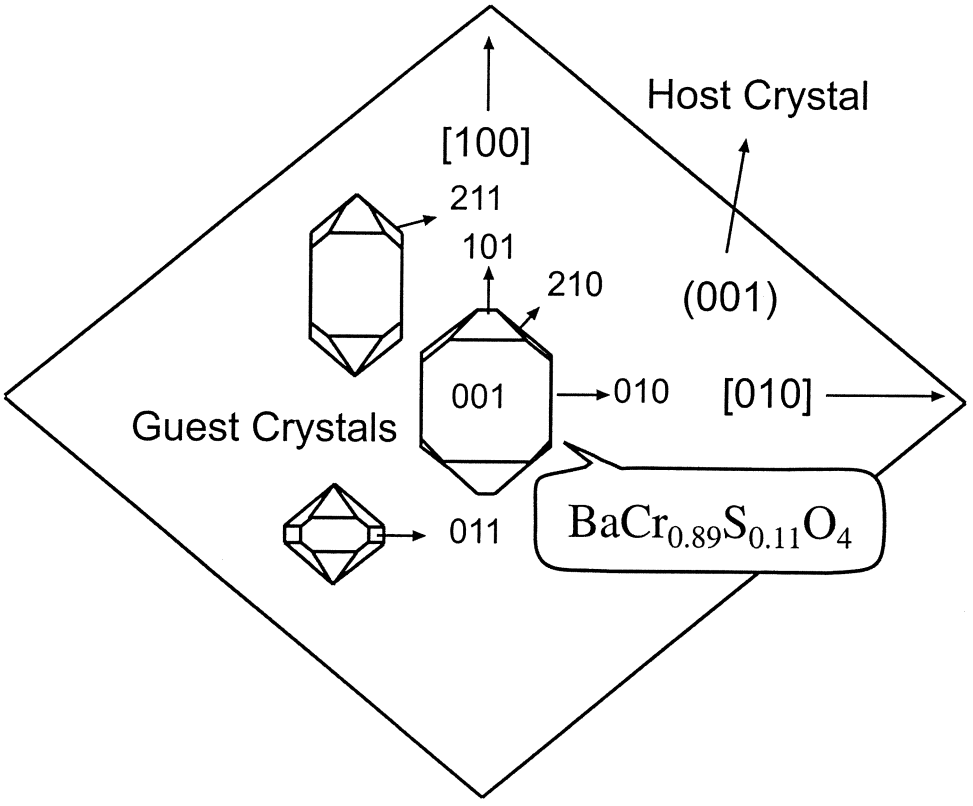

Fig. 5. Crystal morphologies and epitaxial relationships. Three different crystal habits have been represented to illustrate the typical morphologies that can be observed in the precipitate. The three guest crystals have different relative developments of their faces but are all equally oriented on the substrate, with a strict parallelism between [100] and [010] crystallographic directions of substrate and overgrowing crystals.

diffusivity of the ions, but apparently it seems to be as if the pollutants were retarded by the porous medium. In fact, the term "retardation" is widely used by hydrogeologists and geochemists and the use of a "retardation factor" is presently a common option to model transport of pollutants (Tompson and Jackson, 1996). It is worth noting here that the constant K_d as previously defined is dimensionless: within geohydrology, it is more frequent to use $K_d' = \phi \times K_d/\rho_b$ as an "operative" distribution coefficient (Appelo and Postma, 1996), where ϕ and ρ_b are, respectively, the porosity and the bulk medium density.

Here, the "apparent" diffusion coefficients of chromium in quartz-gel and barite-gel composites have been determined from the concentration-time data shown in Figures 2 and 3. With this aim, a computational iterative procedure has been implemented on the basis of the numerical algorithm:

$$C(x, t + \Delta t) = \frac{1}{6}[C(x - \Delta x, t) + 4 \cdot C(x, t) + C(x + \Delta x, t)]. \quad (7)$$

This algorithm is suitable to account for diffusion in finite systems as shown in Figure 1 (Henisch and García-Ruíz, 1986), as long as the following relationship is maintained between Δx and Δt:

$$\Delta t = \frac{1}{6\bar{D}} \times (\Delta x)^2. \quad (8)$$

For the quartz-gel composite, this procedure leads to a value $\bar{D}(QG) = 4.995 \cdot 10^{-6}$ cm^2/s. As we said before, sorption of Cr(VI) on quartz grains seems to be negligible and we can assume that $K_d = 0$ in Eqn. 5. Therefore, the retardation factor $\Re$ is the unity, which means that both "apparent" and "effective" diffusion coefficients have the same value:

$$D_a(QG) = \bar{D}(QG) = 4.995 \times 10^{-6} \text{ cm}^2/\text{s}. \quad (9)$$

The situation is different when chromate ions diffuse through barite-gel composites. In this case there is a strong sorption, and the values of $D_a(BG)$ and $\bar{D}(BG)$ must differ. In fact, the "effective" diffusion coefficient is the "apparent" diffusion coefficient for an equivalent (with the same porosity and tortuosity) unreactive composite. So we can use the operative diffusion coefficient for the unreactive quartz-gel composite to estimate $\bar{D}(BG)$, with the corresponding corrections for porosity and tortuosity—that is,

$$\bar{D}(BG) = \frac{\phi(BG)/\tau_e^2\,(BG)}{\phi(QG)/\tau_e^2\,(QG)} D_a(QG) = 4.915 \times 10^{-6} \text{ cm}^2/\text{s}. \quad (10)$$

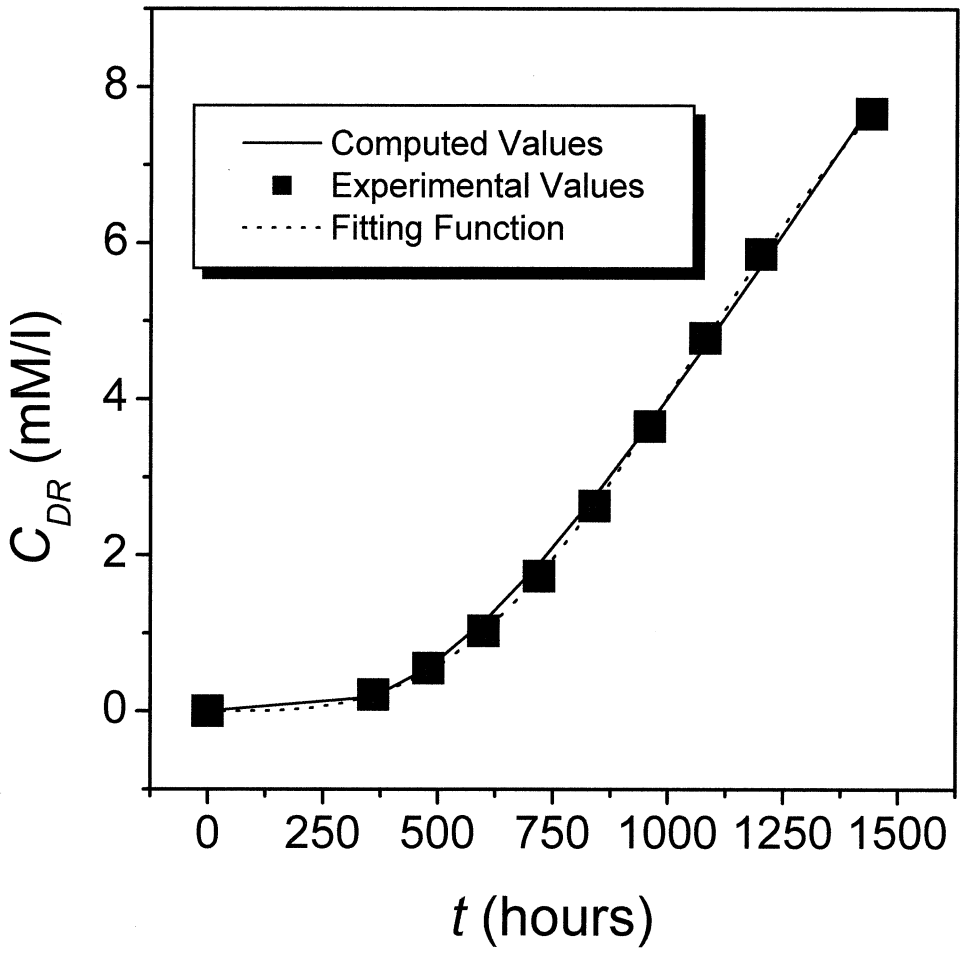

Fig. 6. Concentration evolution in the discharge reservoir for the barite-gel composite. Data points (squares) correspond to experimental values. The dotted line represents the fitting function computed according to Eqn. 2 by using the fitting parameters shown in Table 3. The solid line represents the concentration evolution obtained by iterative computation from the numerical algorithm in Eqn. 7.

Still, to reproduce the experimental results corresponding to barite-gel composites, one must use a factor $K_d = 0.291$ to correct the concentration obtained from each iteration in Eqn. 7. The calculation efficiency is illustrated in Figure 6, where the continuous line represents the concentration evolution in the discharge reservoir obtained from the iterative computation for this value of K_d. The data points correspond to experimental values and the dotted line represents the fitting function computed according to Eqn. 2 by using the fitting parameters shown in Table 3. As can be observed, there is a good agreement between diffusion model and experimental data. Finally, we obtain the apparent diffusion coefficient

$$D_a(\mathrm{BG}) = \frac{\bar{D}(\mathrm{BG})}{1 + K_d} = 3.807 \times 10^{-6}\ \mathrm{cm^2/s}. \qquad (11)$$

So in the case of the barite-gel composite, the sorption reaction slows down the diffusion process by a factor $\Re = 1 + K_d = 1.291$. This factor is not very high because of the moderate tendency of CrO_4^{2-} to partition into barite. In fact, the dimensionless sorption factor K_d is a complex measure that depends on the bulk medium characteristics (reactive surface area of mineral per unit bulk volume of porous medium and porosity) and on more fundamental properties such as the affinity of the substituting ion for the solid solution under the conditions of interest (Tesoriero and Pankow, 1996). For the $Ba(CrO_4,SO_4)$-H_2O system, this affinity can be expressed in terms of a distribution coefficient defined as

$$D_{Cr/S} = \frac{X_{BaCrO_4}/[CrO_4^{2-}]}{X_{BaSO_4}/[SO_4^{2-}]}, \qquad (12)$$

where the terms within brackets are the activities of the aqueous ions, whereas X_{BaCrO_4} and X_{BaSO_4} are, respectively, the solid-phase mole fractions of end members $BaCrO_4$ and $BaSO_4$. At equilibrium, for an ideal solid solution, Eqn. 12 becomes

$$(D_{Cr/S})_{eq} = \frac{K_{BaSO_4}}{K_{BaCrO_4}}, \qquad (13)$$

where K_{BaCrO_4} and K_{BaSO_4} are the thermodynamic solubility

products of the end members. By using end member pK's of 9.98 for barite (Blount, 1977) and 9.67 for $BaCrO_4$ (Smith and Martell, 1976), we have $(D_{Cr/S})_{eq} = 0.49 < 1$, which indicates a moderate preferential partitioning of the less soluble sulfate towards the solid phase. Assuming this equilibrium value, to precipitate a solid solution of composition $BaCr_{0.89}S_{0.11}O_4$, the relation $[CrO_4^{2-}] = \{0.89/(0.11 \times 0.49)\} \times [SO_4^{2-}]$ should be maintained between the aqueous activities of the substituting ions, i.e., the aqueous activity of chromate ions should be 16.512 times higher than the aqueous activity of sulfate ions.

However, one must be careful in applying equilibrium distribution coefficients to account for processes of precipitation of solid solutions that can occur at a certain supersaturation (Lorens, 1981; Prieto et al., 1993, 1997; Pina et al., 2000). One of the main differences between growth in gel media and growth from free solutions lies in the degree of supersaturation needed to start nucleation. Porous media are very effective at moderating nucleation frequency (Prieto et al., 1994; Putnis et al., 1995) and, consequently, precipitation begins always at a higher supersaturation level, compared with nonconfined aqueous solutions. So Fernández-González et al. (1999) find nonequilibrium distribution coefficients in the range $0.67 < D_{Cr/S} < 0.96$ for homogeneous three-dimensional nucleation of $Ba(SO_4,CrO_4)$ in gels. This means that at high supersaturations there is less chance for thermodynamically based selectivity effects to be exerted, and so $D_{Cr/S}$ increases towards the unity—that is, the substituting ions incorporate to the solid in a stoichiometric proportion that tends to approximate that of the aqueous phase.

In the present experiments, we are dealing with nonhomogeneous surface nucleation and a low supersaturation threshold is to be expected to start nucleation. However, the fact that the epitaxial precipitate consists of three-dimensional crystallites indicates a Volmer-Weber mechanism of formation, which is typical for "weak" adhesion of a crystal on the substrate (Chernov, 1984). This mechanism occurs for $\Delta\alpha > 0$, where $\Delta\alpha$ is the variation of the free energy per unit area of the substrate interface associated with the replacement of the substrate-fluid interface by the substrate-crystallite interface plus the crystallite-fluid interface. The stronger the adhesion of the crystal on the substrate is, the smaller are $\Delta\alpha$ and the work of formation of the nuclei, and the smaller is the deviation from equilibrium required for nucleation. So the third step in the sorption process (the reaction between the released solute and the diffusing chromate to form epitaxial solid-solution nuclei) implies that the pore fluid must reach a certain degree of supersaturation with respect to the crystallizing phase. Although a quantitative evaluation of this supersaturation level is impossible in this "black box" system, one can establish the possible limiting scenarios for the saturation state.

For the system $Ba(CrO_4,SO_4)$-H_2O, the saturation state of a given aqueous solution depends on the solid-phase composition that one considers and can be quantified according to the expression (Fernández-González et al., 1999):

$$\beta(x) = \frac{[Ba^{2+}]\,[CrO_4^{2-}]^x\,[SO_4^{2-}]^{(1-x)}}{(K_{BaCrO_4} \times x)^x\,(K_{BaSO_4} \times (1-x))^{(1-x)}}, \qquad (14)$$

where the solid solution is assumed to be ideal, being $x = X_{BaCrO_4}$ and $1 - x = X_{BaSO_4}$. Therefore, in establishing the saturation state of a particular aqueous solution one must compute the $\beta(x)$ function for the entire compositional range from $x = 0$ to 1. Thus, Figure 7 shows a series of $\beta(x)$ functions computed according to Eqn. 14 with the help of a speciation model for the aqueous solution. All these curves correspond to aqueous solutions that satisfy the following restraints:

(1) $[CrO_4^{2-}]/[SO_4^{2-}] = 16.512$, that is to say, the ratio between the aqueous activities of the substituting ions is that one required to precipitate $BaCr_{0.89}S_{0.11}O_4$ solids, on the assumption that the distribution coefficient is equal to the equilibrium one (0.49).

(2) The total molalities of barium and sulfate are exactly alike, which means that all barium and sulfate aqueous species arise from the dissolution of the virtually stoichiometric barite grains.

(3) The maximum value that can be attained for $\beta(0)$ is the unity, which corresponds to saturation for pure barite.

The upper solid curve in Figure 7 corresponds to an aqueous solution that has reached saturation, $\beta(0) = 1$, for the barite end member. Obviously, this curve represents the "upper limit" of supersaturation that can be reached by an aqueous solution that fulfills the restraints 1, 2, and 3. On the contrary, the lower solid curve represents the $\beta(x)$ function for an aqueous solution that is at saturation, $\beta(0.89) = 1$, for $BaCr_{0.89}S_{0.11}O_4$. So to precipitate solids under the specified restraints, the supersaturation function of the aqueous solution must be intermediate, i.e., both solid curves represent the limiting scenarios from which $BaCr_{0.89}S_{0.11}O_4$ solids could have nucleated.

The previous approach has, however, an incongruity: restraint 1 involves assuming $D_{Cr/S} = 0.49$; that is, we are using an equilibrium distribution coefficient to asses limiting conditions of supersaturation (nonequilibrium). In reality, in nonequilibrium conditions, the nuclei will tend to be enriched in the most soluble $BaCrO_4$ end member, and the "effective" $D_{Cr/S}$ will increase with increasing supersaturation (Fernández-González et al., 1999). Therefore, one must still estimate the effect of increasing $D_{Cr/S}$ on the position of the upper limiting $\beta(x)$ function. This effect is shown in Figure 8, where the limiting $\beta(x)$ functions computed for $D_{Cr/S} = 0.67$ and 0.96 are displayed. Both curves plot below the obtained for 0.49, which means that the upper limiting $\beta(x)$ function decays as the distribution coefficient separates from the equilibrium value. Therefore, the maximum supersaturation of the pore fluid from which the crystallites shown in Figure 4 could have nucleated corresponds to the maximum of the upper curve in Figures 7 and 8—that is, $\beta(0.89) = 9.087$. This value is orders of magnitude lower than the values observed for homogeneous three-dimensional nucleation of $Ba(SO_4,CrO_4)$ in gels (Fernández-González et al., 1999), which means that the barite substrate catalyses strongly the nucleation of the overgrowing $BaCr_{0.89}S_{0.11}O_4$ crystals.

It is worth noting that the maxima of the curves computed for nonequilibrium distribution coefficients do not correspond to $X_{BaCrO_4} = 0.89$, the composition of the nucleating crystal. This is just an intrinsic feature of nonequilibrium partitioning: the precipitate composition is not that for which the system is more supersaturated but that one for which nucleation is more favored by kinetic reasons.

Finally, the fact that the nuclei composition always lies in a narrow range around $X_{BaCrO_4} = 0.89$ is easy to understand if

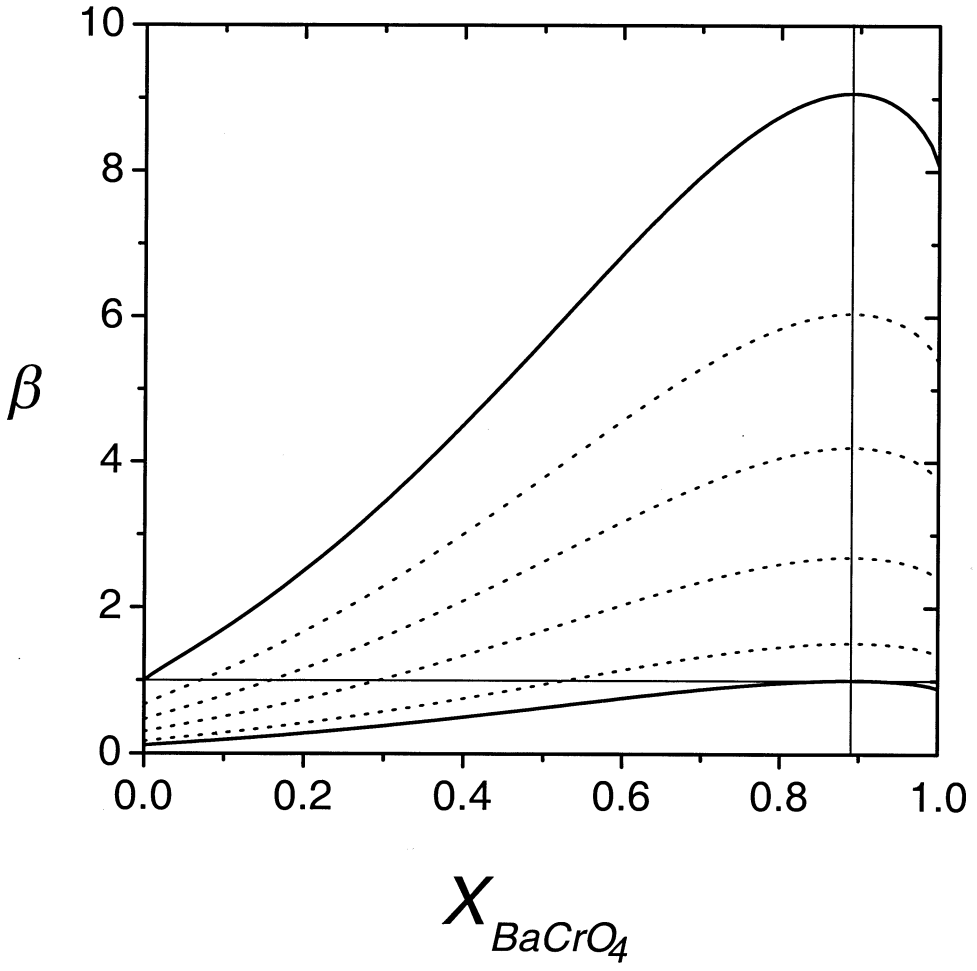

Fig. 7. Supersaturation $\beta(x)$ functions computed according to the restraints 1, 2, and 3 as defined in the text. The upper solid curve corresponds to an aqueous solution that is saturated, $\beta(0) = 1$, for the barite end member. The lower solid curve represents the $\beta(x)$ function for an aqueous solution that is at saturation, $\beta(0.89) = 1$, for $BaCr_{0.89}S_{0.11}O_4$.

one considers that in this experimental system all barium and sulfate ions come from dissolution of barite grains. This means that the supply of these ions to the aqueous solution is virtually the same anywhere in the diffusion column. At a given position, the supersaturation threshold for nucleation is attained when the concentration of chromate ions diffusing from the reservoir reaches a certain critical level. This critical concentration appears to be nearly a constant, so that the ratio $[CrO_4^{2-}]/[SO_4^{2-}]$ is always similar when nucleation occurs. For the same reason, a moderate change in the initial concentration of Na_2CrO_4 in the reservoir has no significant implications on the precipitate compositions. Small compositional variations could arise as a result of local phenomena but an additional source (or sink) of sulfate (or barium) ions is necessary to obtain precipitates with significant differences in Cr/S ratios. Obviously, this compositional outcome is specific for the composite used in this work: a change in the transport properties (porosity, tortuosity, etc.) of the column will affect the supersaturation threshold needed for nucleation and, consequently, the critical concentration of chromate at the nucleation time.

5. CONCLUSIONS AND ENVIRONMENTAL IMPLICATIONS

The introduction of this paper postulated two assessments that have focused the present research: first, immobilization of aqueous Cr(VI) does not necessarily involve reduction to the less mobile and toxic Cr(III), and second, the use of a gel medium in metal-sorption experiments may facilitate the characterization of the sorbed phase, at least when sorption occurs by surface precipitation of a metal-bearing solid. In our opinion, the resulting experiments work to confirm both assessments.

A simple study of transport behavior may reveal a significant immobilization of a pollutant by sorption on certain mineral surfaces but is not enough for remediation purposes. The knowledge of what sorbed phases are present (as well as their mechanism of sorption) is an important step in the selection of an appropriated remediation strategy or in studying the fate of a pollutant in the environment. When sorption involves formation of a precipitate, the use of a medium that minimizes the

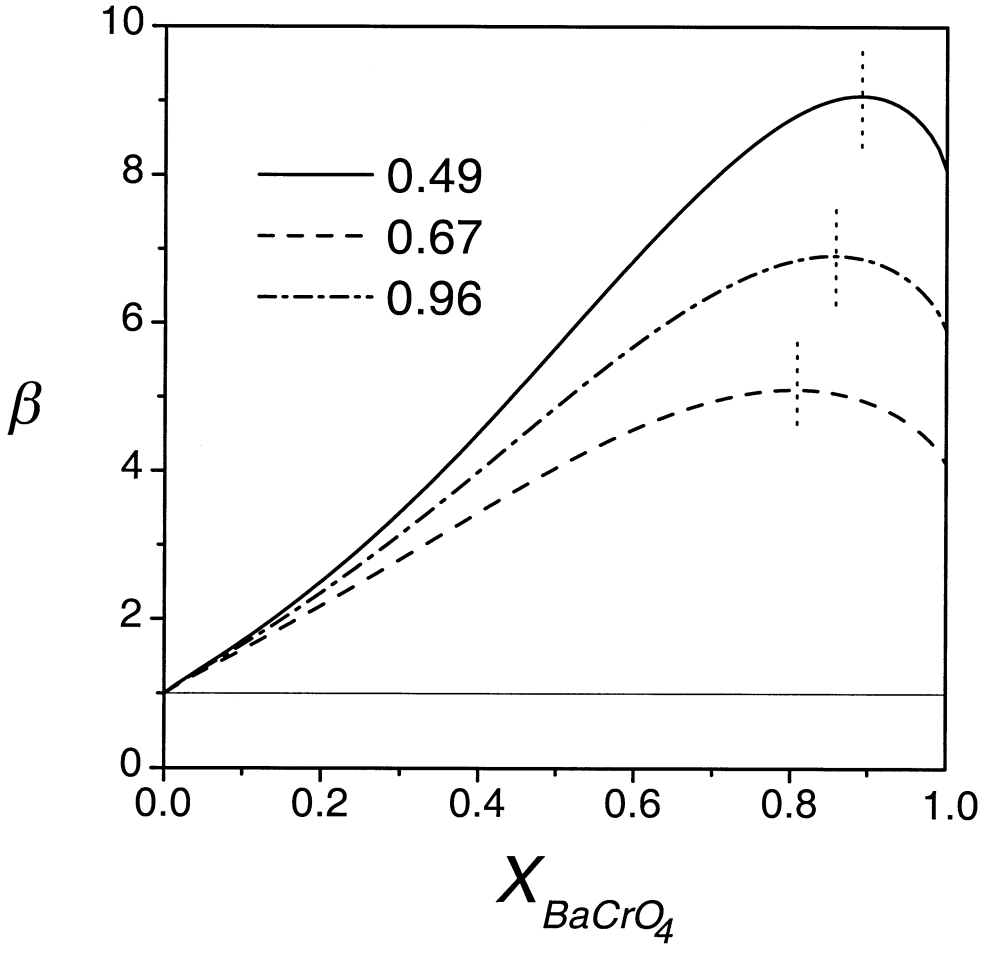

Fig. 8. Supersaturation $\beta(x)$ functions computed by modifying the first restraint for different $D_{Cr/S}$ distribution coefficients (0.49, 0.67, and 0.96). In all cases, the functions correspond to aqueous solutions that are at saturation, $\beta(0) = 1$, for the barite end member (maximum value for $\beta(0)$ in the third restraint) and that satisfy the second restraint.

nucleation density may be an advantageous tool to facilitate this second task.

Nucleation from aqueous solutions is a probabilistic phenomenon that depends on both the supersaturation and the energy barrier encountered by the growth units for transport from the bulk solution to subcritical clusters (Walton, 1969). During cluster formation, its immediate vicinity becomes poor in the dissolved substance, decreasing the probability of formation of a stable nucleus: the disappearance of a subcritical cluster is ensured if no exchange brings new growth units into its vicinity. In a gel, new growth units can enter this region only by diffusion, which is a very slow process in a medium where the fluid is trapped in small pores connected by tortuous ways. For this reason gels reduce the nucleation density and offer certain research opportunities that experiments on crystallization in free solutions cannot provide. Here, we have illustrated these possibilities by looking at the sorption of Cr(VI) on the surface of barite crystals: provided that sorption occurs by surface precipitation of Cr-bearing solids, the low nucleation density allows obtaining precipitating individuals that are large enough to be analyzed in a scanning electron microscope. In contrast, when similar sorption experiments are carried out in free solutions, the substrate becomes covered by a fine precipitate that is complicated to characterize.

The present results clearly show that precipitation of $Ba(SO_4,CrO_4)$ on barite can cause a significant retardation in the mobility of toxic chromate species. The question is to which extent solid-solution partitioning to barite is relevant for remediation purposes. One can find, however, that the previous outcomes have also some keys to answer this question:

(1) In the presence of chromate ions an aqueous solution saturated for barite is always supersaturated ($\beta > 1$ in Eqn. 14) for a certain range of $Ba(SO_4,CrO_4)$ solid solutions, even if chromate ions are present in trace levels. This is an implicit consequence of the fact that barite and barium chromate form a complete (nearly ideal) solid-solution series. Under oxic conditions, if 0.1 ppm of chromium (the EPA Maximum Contaminant Level) are added to an aqueous solution saturated for barite, the solution becomes supersaturated for a series in the range $0 < X_{BaCrO_4} < 0.23$, with a maximum $\beta(x) = 1.083$ at $X_{BaCrO_4} = 0.08$.

(2) Although the value $\beta(0.08) = 1.083$ of this maximum is low for homogeneous three-dimensional nucleation, it can be considered high enough for growth of $BaCr_{0.08}S_{0.92}O_4$ on a

barite substrate because of the insignificant structural misfit ($f_{[100]}$ = 0.0014% in Eqn. 3) between both phases.

(3) The experiments described in this work demonstrate that barite catalyses strongly the surface nucleation of $Ba(SO_4,CrO_4)$ solid solutions. Even in the extreme case of chromium-rich crystals ($f_{[100]}$ = 2.33%) precipitating on barite immersed in a nucleation-suppressing gel medium, the supersaturation threshold seems to be quite moderate. This means that an aqueous solution supersaturated for a range of $Ba(SO_4,CrO_4)$ solid solutions cannot remain metastable for a long time in the presence of barite. The system will approximate in due course to equilibrium by epitaxial overgrowth of crystallites of solid solution.

The previous considerations clearly confirm that immobilization of aqueous Cr(VI) does not necessarily involve the use of reducing agents to change the oxidation state to Cr(III). Potential remedial options for in situ treatment of natural waters contaminated with chromium could include the use of barite hindrances (permeable barriers, reactive zones, etc.) under oxic conditions. On the other hand, recent research findings seem to support that natural attenuation of Cr(VI) is a viable option in many soils and natural waters. This hypothesis is based on the existence of natural reductants that can transform the hexavalent form of chromium to the less mobile trivalent form. For instance, Fe(II) is one of the more ubiquitous potential reducing agents for chromate in natural systems (Ilton et al., 1997). Ferrous iron is abundant in many suboxic and anoxic soils and sediments, which suggests that reduction of Cr(VI) by Fe(II) can be important to chromium geochemistry in suboxic or anoxic natural waters (Sedlak and Chang, 1997; Pettine et al., 1998). The question is to which extent sorption of chromate on barite could contribute in a similar way to natural attenuation of Cr(VI) in oxic aqueous environments.

A review by Hanor (2000) shows to what point barite is ubiquitous in natural environments. Barite is a widespread component of oceanic sediments and most oceanic waters are nearly saturated with respect to this mineral. The solubility of barite is so low that natural waters can exist that have significant concentrations of either dissolved barium or sulfate, but not both. In fact, buffering by barite restrains the concentration of barium in many crustal waters, including some shallow meteoric groundwater systems. This buffering is also an important control on the concentration of barium in drinking water supplies. So all data indicate that barite is a powerful geochemical phase and, consequently, natural attenuation of Cr(VI) by sorption/precipitation on or with barite could be a possibility in many aqueous environments. However, there are not many works that hypothesize this possibility to explain actual occurrences. Kersten et al. (1998) postulated that coprecipitation and solid solution formation with barite could explain the low chromate concentration in leachates of a municipal solid waste incineration bottom-ash landfill. This hypothesis was verified by measurement of Cr in secondary barite precipitates found in aged bottom ash via wavelength dispersive electron microprobe X-ray microanalysis. In the same way, Frutchter et al. (cited by Kersten et al., 1998) suggested by saturation index calculations that chromate precipitation with barite could be an explanation for a similar low chromate concentration observed in some coal fly leachates.

In summary, the present results demonstrate that precipitation of $Ba(SO_4,CrO_4)$ solid solutions may be an option to control the concentration of Cr(VI) in oxic environments. Natural attenuation of chromium is likely to occur by this mechanism in some aqueous environments and this possibility should considered in environmental assessment of Cr(VI) behavior. Neglecting to consider such solid solution formation will lead to overestimates of the availability and mobility of Cr(VI).

Acknowledgments—This work was supported by DGES (Dirección General de Enseñanza Superior, Ministry of Science and Technology; Spain; grant BTE2000-0300 and by the European Commission (contract HPRN-CT-2000-0058) . We thank two anonymous reviewers for their insightful comments. We also thank associate editor E. Merino for his constructive comments, which improved the manuscript.

Associate editor: E. Merino

REFERENCES

Appelo C. A. J. and Postma D. (1996) *Geochemistry, Groundwater and Pollution.* A. A. Balkema.

Blount C. W. (1977) Barite solubilities and thermodynamic quantities up to 300°C and 1400 bars. *Am. Mineral.* **62,** 942–957.

Brown G. E., Parks G. A., and O'Day P. A. (1995) Sorption at mineral-water interfaces: Macroscopic and microscopic perspectives. In *Mineral Surfaces* (eds. D. J. Vaughan and R. A. D. Pattrick), pp. 129–183. Chapman & Hall.

Chernov A. A. (1984) *Modern Crystallography III: Crystal Growth.* Springer-Verlag, Berlin.

Chiarello R. P., Sturchio N. C., Grace J. D., Geissbuhler P., Sorensen L. B., Cheng L., and Xu S. (1997) Otavite–calcite solid solution formation at the calcite–water interface studied in situ by synchrotron X-ray scattering. *Geochim. Cosmochim. Acta* **61,** 1467–1474.

Crank J. (1975) *The Mathematics of Diffusion*. Clarendon Press.

Davis J. A., Fuller C. C., and Cook A. D. (1987) A model for trace metal sorption processes at the calcite surface: Adsorption of Cd^{2+} and subsequent solid solution formation. *Geochim. Cosmochim. Acta* **51,** 1477–1490.

Dudley L. M., McLean J. E., Sims R. C., and Jurinak J. J. (1988) Sorption of copper and cadmium from the water soluble fraction of an acid mine waste by two calcareous soils. *Soil Sci.* **145,** 207–214.

Fernández-González A., Martín-Díaz R., and Prieto M. (1999) Crystallisation of $Ba(SO_4,CrO_4)$ solid solutions from aqueous solutions. *J. Cryst Growth.* **200,** 227–235.

Fuller C. C. and Davis J. A. (1987) Processes and kinetics of Cd^{2+} sorption by a calcareous aquifer sand. *Geochim. Cosmochim. Acta* **51,** 1491–1502.

Grathwohl P. (1998) *Diffusion in Natural Porous Media: Contaminant Transport, Sorption/Desorption and Dissolution Kinetics*. Kluwer.

Hanor J. F. (2000) Barite-celestine geochemistry and environments of formation. In *Sulfate Minerals* (eds. C. N. Alpers, J. L. Jambor, and D. K. Nordstrom). *Reviews in Mineralogy*, Vol. 40, pp. 193–276. Mineralogical Society of America.

Hauff P. L., Foord E. E., Rosemblum S., and Hakki W. (1983) Hashemite, $Ba(Cr,S)O_4$, a new mineral from Jordan. *Am. Mineral.* **68,** 1223–1225.

Henisch H. K. (1988) *Crystals in Gels and Liesegang Rings*. Cambridge University Press.

Henisch H. K. and García-Ruíz J. M. (1986) Crystal growth in gels and Liesegang ring formation. I Diffusion relationships. *J. Cryst. Growth* **75,** 195–202.

Ilton E. S., Veblen D. R., Moses C. O., and Raeburn S. P. (1997) The catalytic effect of sodium and lithium ions on coupled sorption-reduction of chromate at the biotite edge-fluid interface. *Geochim. Cosmochim. Acta* **61,** 3543–3563.

Kersten M., Schulz-Dobrick B., Lichtensteiger T., and Johnson C. A. (1998) Speciation of Cr in leachates of a MSWI bottom ash landfill. *Environ. Sci. Technol.* **32,** 1398–1403.

Lefaucheux F. and Robert M. C. (1994) Crystal growth in gels. In

Handbook of Crystal Growth 2 (ed. D. T. J. Hurle), pp. 1271–1303. Elsevier.

Lorens R. B. (1981) Sr, Cd, Mn and Co distribution coefficients in calcite as a function of calcite precipitation rate. *Geochim. Cosmochim. Acta* **45,** 553–561.

Miyake M., Minato I., Morikowa H., and Iwai S. (1978) Crystal structures and sulphate force constants of barite, celestite, and anglesite. *Am. Mineral.* **63,** 506–510.

Nriagu J. O. (1988) Production and use of chromium. In *Chromium in the Natural and Human Environments* (eds. J. O. Nriagu and E. Nieboer), pp. 81–104. Wiley.

Oelkers E. H. (1996) Physical and chemical properties of rocks and fluids for chemical mass transport calculations. In *Reactive Transport in Porous Media* (eds. P. C. Lichtner, C. I. Steefel, and E. H. Oelkers). *Rev. Mineral.* **34**, 131–191.

Peterson M. L., Brown G. E., Parks G. A., and Stein C. L. (1997) Differential redox and sorption of Cr(III/VI) on natural silicate and oxide minerals: EXAFS and XANES results. *Geochim. Cosmochim. Acta* **61,** 3399–3412.

Pettine M., D'Ottone L., Campanella L., Millero F. J., and Passino R. (1998) The reduction of chromium (VI) by iron (II) in aqueous solutions. *Geochim. Cosmochim. Acta* **62,** 1509–1519.

Pina C. M., Enders M., and Putnis A. (2000) The composition of solid solutions crystallising from aqueous solutions: The influence of supersaturation and growth mechanisms. *Chem. Geol.* **168,** 195–210.

Prieto M., Putnis A., and Fernández-Díaz L. (1990) Factors controlling the kinetics of crystallization: Supersaturation evolution in a porous medium. Application to barite crystallization. *Geol. Mag.* **127,** 485–495.

Prieto M., Putnis A., and Fernández-Díaz, L. (1993) Crystallization of solid solutions from aqueous solutions in a porous medium: Zoning in (Ba, Sr)SO_4. *Geol. Mag.* **130,** 289–299.

Prieto M., Putnis A., Fernández-Díaz L., and López-Andrés S. (1994) Metastability in diffusing-reacting systems. *J. Cryst. Growth.* **142,** 225–235.

Prieto M., Fernández-González A., Putnis A., and Fernádez-Díaz L. (1997) Nucleation, growth, and zoning phenomena in crystallizing (Ba,Sr)CO_3, Ba(SO_4,CrO_4), (Ba,Sr)SO_4, and (Cd,Ca)CO_3 solid solutions from aqueous solutions. *Geochim. Cosmochim. Acta* **61,** 3383–3397.

Putnis A., Prieto M., and Fernández-Díaz L. (1995) Fluid supersaturation and crystallization in porous media. *Geol. Mag.* **132,** 1–13.

Reeder R. J. (1996) Interaction of divalent cobalt, zinc, cadmium, and barium with the calcite surface during layer growth. *Geochim. Cosmochim. Acta* **60,** 1543–1552.

Sedlak D. L. and Chan P. G. (1997) Reduction of hexavalent chromium by ferrous iron. *Geochim. Cosmochim. Acta* **61,** 2185–2192.

Smith R. M. and Martell A. E. (1976) *Critical Stability Constants.*Vol. 4, *Inorganic Complexes.* Plenum Press.

Sposito G. (1986) Distinguishing adsorption from surface precipitation. In *Geochemical Processes of Mineral Surfaces* (eds. J. A. Davis and K. Hayes), pp. 217–228. Symposium Series 323. American Chemical Society.

Stipp S. L., Hochella M. F., Parks G. A., and Leckie J. O. (1992) Cd^{2+} uptake by calcite, solid-state diffusion, and the formation of solid-solution: Interface processes observed with near-surface sensitive techniques (XPS, LEED, and AES). *Geochim. Cosmochim. Acta* **56,** 1941–1954.

Tesoriero A. J. and Pankow J. F. (1996) Solid solution partitioning of Sr^{2+}, Ba^{2+}, and Cd^{2+} to calcite. *Geochim. Cosmochim. Acta* **60,** 1053–1063.

Tompson A. F. B. and Jackson K. J. (1996) Reactive transport in heterogeneous systems: An overview. In *Reactive Transport in Porous Media* (eds. P. C. Lichtner, C. I. Steefel, and E. H. Oelkers). *Rev. Mineral.* **34**, 269–310.

Walton A. G. (1969) Nucleation in liquids and solutions. In *Nucleation* (ed. A. C. Zettelmoyer), pp. 225–307. Marcel Dekker.

Zachara J. M., Cowan C. E., and Resch C. T. (1991) Sorption of divalent metals on calcite. *Geochim. Cosmochim. Acta* **55,** 1549–1562.